

Study of cluster states in nuclei using nuclear reactions

Chinmay Basu*

Nuclear Physics Division, Saha Institute of Nuclear Physics, 1/AF Bidhan nagar, Kolkata-700064, INDIA

*email: chinmay.basu@saha.ac.in

Light nuclei such as ^8Be , ^{12}C , ^{16}O , ^{24}Mg etc. exhibit properties that can be explained by assuming alpha cluster constituents in them. The experimental evidence of such clustering states can be obtained from elastic scattering, transfer and breakup reactions. Measurements of the resonant breakup angular distributions and comparison with advanced breakup theory (such as the Continuum Discretized Coupled Channel (CDCC) calculations) provide information of the spectroscopic properties of alpha cluster states. We describe results of experiments performed to study the $\alpha+^{14}\text{C}$ and other possible heavy ion structure of ^{18}O using the RPS method. Some higher lying cluster states of ^{18}O have been observed in this study. High quality RPS data for ^{16}O breakup from ^{208}Pb target has been analyzed in terms of the CDCC formalism to extract the alpha spectroscopic factor and Asymptotic Normalization Constant (ANC) of the ^{16}O ground state. The same study has been extended to the case of light target (^{27}Al). These properties are useful for the study of the $^{12}\text{C}(\alpha,\gamma)$ reaction that is a very important reaction in nuclear astrophysics. Besides light nuclei α clustering has been predicted in heavy nuclei such as ^{212}Po . Recent elastic scattering data of alpha particles from ^{208}Pb provide information about the $\alpha+^{208}\text{Pb}$ potential that can be used to generate the cluster states in the ^{212}Po system. Besides, some results about the subthreshold states of ^{16}O using alpha transfer reactions are also described.

1. Introduction

The properties of the nucleus are generally well described by the neutron proton picture. However, certain properties indicate a possible clustering of the constituent nucleons inside the nucleus. Alpha clustering is the most common form of such phenomena. This is due to the relatively larger binding energy of the alpha nucleus. Light nuclei such as ^8Be , ^{12}C , ^{16}O , ^{24}Mg etc. exhibit properties that can be explained by assuming alpha cluster constituents in them [1]. They can be either described in terms of N alpha particles or a alpha+core structure. In some nuclei (e.g. ^9Be) the presence of a neutron along with alpha-particles stabilizes the nucleus as in a covalent bond in atomic systems. There may be also heavy ion cluster structure such as $^{12}\text{C}+^{12}\text{C}$ in ^{24}Mg or alpha+ ^{12}C in ^{16}O [1]. The cluster structure of such light nuclei was first studied theoretically by a number of workers during the 1950s and 1960s. Fred Hoyle [2] suggested a 7.65 MeV 0^+_2 state for ^{12}C to explain its abundance in stars. This state is a resonance state generated by 3 alpha particles forming the ^{12}C nucleus. Subsequently Japanese scientist Ikeda [3] suggested that clustering states appear just above the corresponding cluster breakup thresholds.

The experimental observation of these states are however difficult. They can be studied using either elastic scattering [4], transfer [5] or breakup reactions [6]. The early investigations involved measurement of scattering resonances as a function of bombarding energy. Resonances are marked by the increased yield at the resonance energies. However in this method it was difficult to separate contributions from other reaction mechanisms.

The most direct evidence of cluster states were developed in the 80's from a technique using breakup reactions [7]. This technique known as resonant particle spectroscopy (RPS) has then been

applied for many nuclei. However, such measurements in many cases are limited and need further study. For example, alpha conjugate nuclei ($N\alpha$ nuclei where N is an integer) have been studied more extensively than the alpha non conjugate systems. An interesting nucleus to study is the alpha non conjugate nucleus ^{18}O . This nucleus has been theoretically predicted to have a prominent $\alpha+^{14}\text{C}$ cluster structure. Rae and Bhowmik [8,9] first studied the cluster structure of ^{18}O experimentally using the RPS method through the resonant breakup reaction $^{12}\text{C}(^{18}\text{O}, ^{14}\text{C}\alpha)$ at $E(^{18}\text{O}) = 82$ MeV. Very recently, the same reaction was studied at a much higher energy by Yildiz et al. at 130 MeV [10]. Curtis et al. (at 120 MeV) [11] and Ashwood et al. (at 148 and 152 MeV) [12] have also reported the cluster states of ^{18}O but using different targets. Though both the studies reported a number of cluster states, and deduced their energies, spin and parities some of the high lying states of ^{18}O produced by transfer reaction $^{14}\text{C}(^6\text{Li}, d)^{18}\text{O}$ [13] could not be observed in these studies and were also not observed in inelastic excitation of ^{18}O through other reactions. Moreover, the spin assignments of the cluster states of ^{18}O are ambiguous and demand more measurements at other energies in order to resolve the ambiguities.

Recently [14] a measurement of alpha cluster states of ^{18}O through the resonant breakup reaction $^{12}\text{C}(^{18}\text{O}, ^{14}\text{C}\alpha)$ at $E(^{18}\text{O}) = 94.5$ MeV were performed where no earlier measurements exist. The chosen projectile energy is in between that of the earlier experiments and may be fruitful in producing resonant breakup (more probable at lower energy) as well as higher lying excited states (more probable at higher energy). We make a Continuum-Discretized Coupled Channel (CDCC) [15] analysis of the breakup angular distribution to investigate the reaction process. In the present

work, we observed a number of excited states in the range 15.8-17.3 MeV.

In recent times [16,17], breakup reactions have been utilized to extract the Asymptotic Normalization Coefficient (ANC) of nuclear states, useful in astrophysics. The feasibility of this method lies in the peripheral nature of the breakup reaction under study and how well the breakup process is analysed by some appropriate theory. The continuum-discretized-coupled channel (CDCC) method describes breakup reaction in the most appropriate way by considering the continuum and the effect of nuclear and Coulomb contribution on an equal footing.

Therefore, the use of CDCC theory provides an improved breakup reaction analysis and hence the ANC extracted in this method is expected to be more reliable. The CDCC + ANC approach also enables one to investigate the effect of continuum-continuum coupling on the extracted ANC. A number of reactions that involve nuclei with low breakup threshold have been studied as for such systems breakup is expected to be more peripheral than for compact nuclei. Important astrophysical reactions viz. ${}^7\text{Be}(p,\gamma)$, ${}^3\text{He}(\alpha,\gamma)$, ${}^{14}\text{C}(n,\gamma)$ have been studied in this method from the breakup of ${}^8\text{B}$ [18], ${}^7\text{Be}$ [19], ${}^{15}\text{C}$ [20] respectively. Particularly, the first reaction has been extensively studied not only because of its astrophysical importance but also due to low proton threshold of the ${}^8\text{B}$ nucleus. Since the CDCC+ANC method have been so far applied mainly to loosely bound nuclei it will be interesting to apply this method to a compact nucleus. Therefore when we started reading the CDCC + ANC approach, we at first thought of applying it to a recent data of ${}^{16}\text{O}$ breakup [21] into alpha particles and ${}^{12}\text{C}$ nuclei. This data was not analysed in terms of the CDCC formalism and it is possible to calculate the ground state ANC and the reduced alpha widths of ${}^{16}\text{O}$ unbound states from this study. These properties of ${}^{16}\text{O}$ states can provide some information relevant to the R-matrix calculation [22] of the astrophysically important ${}^{12}\text{C}(\alpha,\gamma)$ reaction [23]. In this work, we analyze using CDCC theory the resonance breakup of ${}^{16}\text{O}$ through two 2^+ above threshold states (9.84 and 11.52 MeV). The reduced α widths of these unbound states have been already determined from ${}^{12}\text{C}(\alpha,\alpha)$ elastic scattering measurements. It may be mentioned in this connection that the ANC of the important 2^+ subthreshold state (6.913 MeV) of ${}^{16}\text{O}$ has been determined from elastic scattering and peripheral α -transfer reactions. On the other hand the determination of the ${}^{16}\text{O}$ ground state ANC is also necessary and important for understanding the E2 ground-state cross section. As the reduced α width of ${}^{16}\text{O}$ ground state is known to be small, the transfer reaction experiments used in previous studies are not expected to give reliable results for the ground state. Traditional methods to

experimentally determine S_α are the alpha transfer and knockout reactions. The transfer reaction method show large uncertainty in the extracted alpha spectroscopic factor. This is due to the ambiguity in the nuclear interaction potential involved in the DWBA (Distorted Wave Born Approximation) calculations. The knockout reactions on the other hand are restricted to using the nucleus of interest as the target.

The breakup method used in the present work [6] may therefore prove to be more useful for determining the ground state ANC of ${}^{16}\text{O}$. Similar analysis of ${}^{16}\text{O}$ breakup data from a light target ${}^{27}\text{Al}$ at low energies have been done [24]. In spite of a light target, the results of our calculations show good stability for the extracted S_α value with respect to the change in $\alpha+{}^{12}\text{C}$ binding potential.

2. Resonant Particle Spectroscopy (RPS) method

Resonant particle spectroscopy method [7,25] uses the breakup of a projectile in the field of the target. The breakup fragments emitted from a resonant state of the projectile (the nucleus whose cluster states are of interest) are detected in coincidence. The determination of the energy and angle of the two fragments out of the three final products is sufficient. The energy of the third particle can be determined from momentum conservation. However this method is comparatively simple for a two body (cluster+core) structure of the projectile. In case of more than two components the difficulty of the experiment is significantly increased. However, in this work we have only concentrated on the simpler two body structures. In the RPS method for such two body configuration the total energy and the excitation energy are measured. The total energy E_{total} is defined in terms of the energy E_1, E_2, E_3 of the three final fragments as

$$E_{total} = E_1 + E_2 + E_3$$

and the excitation energy as

$$E^* = E_{rel} + S_{12}$$

E_{rel} is the relative energy defined in terms of the energy and angle of 1 and 2 and S_{12} is the separation energy of the breakup particles (1 and 2). The RPS method is more suitable for nuclei with low breakup thresholds and therefore higher breakup cross-sections.

3. Cluster states of ${}^{18}\text{O}$ using RPS method

The experiment was carried out using the 14UD BARC-TIFR Pelletron facility, Mumbai. The beam used was an ${}^{18}\text{O}^{7+}$ (enriched) with an average current of about 24 pA. A 220 $\mu\text{g}/\text{cm}^2$ thick ${}^{12}\text{C}$ target was used which included a 0.35%

impurity of ^{208}Pb . The impurity was determined from the Rutherford scattering of ^{18}O beam (with theoretically known exact cross-section) from the impurity part of the target. The detector setup consisted of a small area ΔE (5 μm) E (3 mm) Si telescope on one side of the beam whereas on the other side of the beam a position sensitive detector (PSD) was placed. The centre of both the telescope and the PSD were at 20° with respect to the beam direction. The telescope and the PSD were at a distance of 89.2 mm and 101.7 mm respectively. The PSD was a 300 mm single area $8 \times 45 \text{ mm}^2$ active region covering a solid angle of 34.5 msr at the target centre. A TAC was generated from the telescope and the PSD signals to gate the data during offline analysis. The energy calibration of the detectors was carried out by elastic scattering from ^{197}Au , ^{12}C , and its impurity ^{208}Pb . The energy resolution of the telescope was 2.4% at 77.8 MeV ^{12}C ions and 50 keV for alpha particles (^{241}Am source) at 5.5 MeV in the PSD.

The total energy spectrum is constructed by measuring the energy of the breakup fragments in coincidence. This measurement requires very high stability performance of the detection system particularly for nuclei that do not have a high breakup cross-section. The total energy spectrum separates the final products in their ground and respective excited states. The excitation energy spectrum obtained from the relative energy is shown in fig. 1 below.

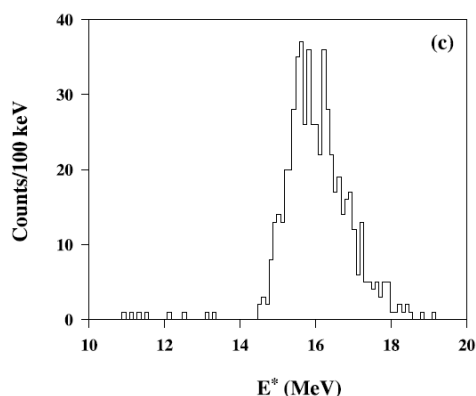


Fig. 1 The excitation energy spectrum of ^{18}O

The states in the higher energy side of the $\alpha+^{14}\text{C}$ excitation spectrum were observed for the ^{18}O nucleus. The angular correlation was also extracted for the 15.8 MeV state. The Legendre polynomial fit of the data (fig. 2) suggest a 5^- spin for the state though systematics show a spin assignment of 1^- . The symbol ψ in fig. 2 represents the angle made by the relative vector of the breakup fragments with respect to the beam axis. The restricted geometry of the detection system in the present work and low breakup cross-section of the state prevents an angular correlation over a

wide range. The angular distribution of the fragments have been also analysed in terms of the Continuum Discretized Coupled Channel (CDCC) theory to study the coupling effects of the various resonant states.

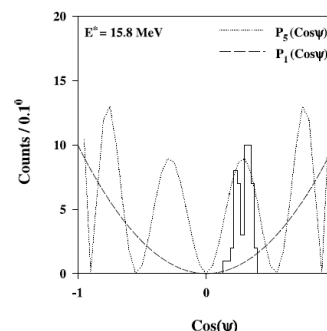


Fig. 2 The intensity distribution of the relative vector angle. The Legendre Polynomial fit with $J=1$ and 5 are shown.

In a different experiment with the same $^{18}\text{O}+^{12}\text{C}$ system at 80 MeV (TIFR-BARC Pelletron) the inclusive heavy ion spectra indicates fragmentation of the projectile. The spectrum for Lithium and Beryllium fragments are shown in figure 3. A Gaussian fit shows the fragments are emitted with beam velocity indicating a fragmentation of the ^{18}O nucleus.

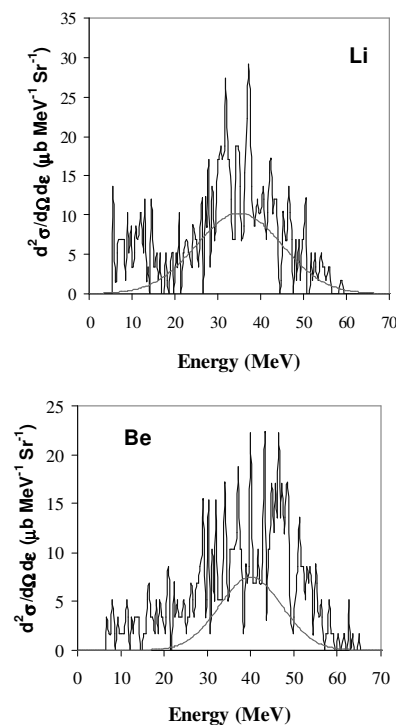


Fig. 3 Inclusive Lithium and Beryllium spectra measured from $^{18}\text{O}+^{12}\text{C}$ reaction at 80 MeV.

4. Cluster states of ^{16}O and application to nuclear astrophysics

Nuclear projectiles having a prominent two body structure may undergo breakup by interaction with the nuclear and Coulomb field of a target. The CDCC theory provides a full quantum mechanical framework to explain the breakup process. In our calculations we have used the CDCC code FRESKO [15] available freely in the web. In FRESKO, breakup is treated as an excitation of the projectile into the continuum, which is optimally discretized into small energy intervals (bins) to define the excited states. Known resonances can be suitably included in the continuum to account for the resonance breakup process. The continuum other than the resonances describes the non-resonant or direct breakup process. A coupled channel equation is then solved by FRESKO involving all bound, resonance and non-resonant states to obtain the breakup cross section.

The starting point of the CDCC+ANC method is a good description of the observed breakup angular distribution. Therefore in our case we need to have a good data set for ^{16}O breakup angular distribution preferably from some heavy target. Recently [21] ^{16}O breakup on ^{208}Pb has been measured at 80 MeV/u at KVI Groningen. The analysis of the KVI data was done in the framework of the coupled channel program ECIS [26] (with the objective of a possible Coulomb dissociation study). The ECIS formalism unlike the CDCC method does not include the effect of the continuum and its coupling which represents the true physical picture of breakup. It may therefore be worthwhile to reanalyze the data in terms of the CDCC formalism and look for the possibility of extracting the α -width and ANC. In the CDCC model space for the ^{16}O resonance breakup reaction the continuum is divided into 8 equal bins in the momentum space upto a maximum relative energy of 8.16 MeV. The 0^+ ground state of ^{16}O and the two resonance states at excitation energy 9.84 MeV (2^+) and 11.52 MeV (2^+) are included in the calculation.

As both the resonances lie in the d wave continuum the energy bins are additionally reconstructed for the $l = 2$ bin (l is the relative angular momentum between the core (^{12}C) and valence particle (α)). The KVI data was taken at incident energy of 1280 MeV and so the initial angular momentum was taken upto 9500h though no significant change in the result could be observed after 2500 h. In the FRESKO calculations three interactions are required to calculate the cross sections. These are the optical potentials between the core (^{12}C) and the target and between the valence particle (α) and the target. The ground state and bin wave functions are generated by a real

potential. The $\alpha+^{208}\text{Pb}$ and $^{12}\text{C}+^{208}\text{Pb}$ optical potentials are required at 320 MeV and 960 MeV respectively. The nearest energy at which optical potentials are available in the literature for these systems are at 340 MeV for $\alpha+^{208}\text{Pb}$ [27] and 1.4 GeV for $^{12}\text{C}+^{208}\text{Pb}$ [28]. The $\alpha+^{12}\text{C}$ binding real potential are adopted from Bertulani [29] and also from the prescriptions of Langanke and Koonin [30]. One form of the potential is of Gaussian shape whereas the other one has a Woods–Saxon form factor.

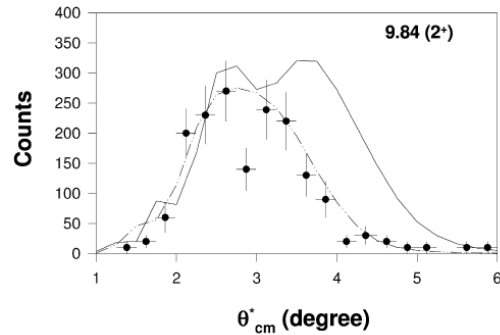


Fig. 4 Comparison of CDCC FRESKO calculations with resonance breakup data. The solid line are calculations with the known alpha width of 0.625 keV [31] and the dashed line with the adjusted alpha width of 62 keV.

The FRESKO calculations using the parameters defined above are compared with the experimental angular distributions in Figs. 4 and 5. The calculations show a good reproduction of shape even in a small angular region. For both the 9.84 MeV and 11.52 MeV state the continuum is restricted to s, p and d waves. Inclusion of $l > 3$ and exclusion of p waves in the calculation affect the results in a very small way. The only observable change occurs only for the 11.52 MeV angular distribution if the $^{12}\text{C}+^{208}\text{Pb}$ potential is changed from a shallow to a deep real potential. However, it is to be noted that the adopted optical potentials for this system is at 1.4 GeV whereas the desired energy at which the potential parameters are required is at 960 MeV. Elastic scattering experiments are therefore required for this system around this energy regime for a better set of optical parameters. Additionally we observe that the adopted interactions are also able to explain the elastic scattering cross section for the $^{16}\text{O}+^{208}\text{Pb}$ system at 1280 MeV. The CDCC calculations are also sensitively dependent on the α -widths of the resonance states of ^{16}O in the present study. These widths are an important constraint in the R-matrix fit of the SE2-factors for the $^{12}\text{C}(\alpha,\gamma)$ reaction. The 9.84 MeV and 11.52 MeV states have interference effects in the accurate prediction of the S-factor and therefore the knowledge of the widths of these states are also important. The full quantum

mechanical CDCC calculation of resonance breakup cross section is sensitive to the particle width of the state. Our calculations with the accepted values of alpha widths existing in the literature show discrepancy at higher angles (Fig. 4 and 5) in the measured angular range. However, this discrepancy could not be improved by varying any of the sensitive parameters in the CDCC model. Interestingly, if we change the alpha width of 9.84 MeV state arbitrarily from 0.625 keV [31] to 62 keV the CDCC predictions show significant improvement (Fig. 4) of the breakup angular distribution through this state. A similar change is observed if the width of 11.52 MeV state is reduced from 71 keV [31] to 15 keV (Fig. 5). However, in the present CDCC formalism ^{16}O is modelled to have a two body $\alpha+^{12}\text{C}$ g.s. structure in all the states involved. This is a limitation, as theoretical calculations [32] indicate multiconfigurational structures such as $\alpha+^{12}\text{C}$ (g.s., 2^+) for ^{16}O states.

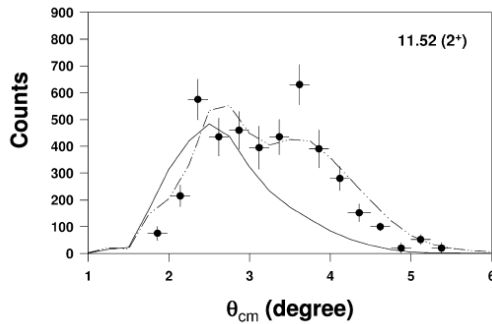


Fig. 5 Comparison of CDCC FRESCO calculations with resonance breakup data. The solid line are calculations with the known alpha width of 71 keV [31] and the dashed line with the adjusted alpha width of 15 keV.

The alpha spectroscopic factor of ^{16}O has been also extracted [24] using the angular distribution data of ^{16}O breakup from a light target (^{27}Al) [33]. Padalino et al [33] measured the inclusive breakup angular distribution of ^{16}O from ^{27}Al target at energies 72 to 125 MeV. This inclusive measurement of ^{16}O breakup cross-section may involve contributions from different types of breakup process. In the CDCC model space for the ^{16}O resonance breakup reaction the continuum is divided into 8 equal bins in the momentum space up to a maximum relative energy of 8.16 MeV. The bins have been constructed for $l=0$ to 4 (l is the relative angular momentum between the core (^{12}C) and valence particle. The $\alpha+^{27}\text{Al}$ and $^{12}\text{C}+^{27}\text{Al}$ optical potentials are adopted respectively from [34] and [35]. The $\alpha+^{12}\text{C}$ binding real potential are adopted from Bertulani [29] and also from the prescriptions of Langanke and Koonin [30]. One form of the potential is of Gaussian shape whereas the other

one has a Woods-Saxon form factor. Fig.6 shows the inclusive breakup angular distribution of C from $^{16}\text{O}+^{27}\text{Al}$ reaction at 72-125 MeV. For this inclusive measurement we consider only non-resonant breakup in the CDCC calculations. The calculations are in good agreement with the data at forward angles below 30° at all energies. However in order to extract the spectroscopic factor that is independent of the potential parameters the breakup process needs to be peripheral. We therefore calculated the breakup angular distribution of ^{16}O for two available binding potentials of $\alpha+^{12}\text{C}$. The CDCC calculations with these two potentials are shown in fig.6 by solid and dashed lines. As can be seen in the figure the two calculations are almost the same at angles below 20° . Therefore it can be said the breakup products that are emitted at these

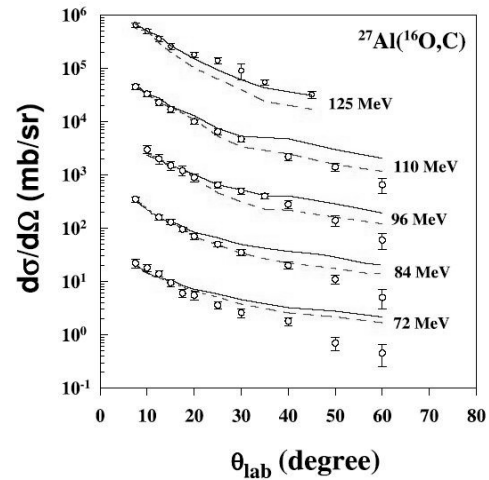


Fig. 6 The inclusive experimental $^{16}\text{O}+^{27}\text{Al}$ breakup angular distributions (symbols) and CDCC calculations with projectile binding potential as Gaussian (solid line) and Wood Saxon (dashed lines).

angles are either insensitive to the binding potential or are sensitive to the potentials at large distance where they are almost the same. It is more realistic to accept the second possibility and so we can consider the breakup process to be peripheral within 20° . The alpha spectroscopic factors in this work are therefore extracted at 10° for all energies. In fig.7 (a) and (b) we show the variation of spectroscopic factor with respect to the incident energy and single particle ANC b . The variation in b represents a variation in the single particle binding potential as the former is obtained by a normalization of the ground state cluster wave function with respect to the Whittaker function at large radial separation. In almost all the cases the S_α change very little with the change in b . It is therefore interesting to study this aspect in more details in future.

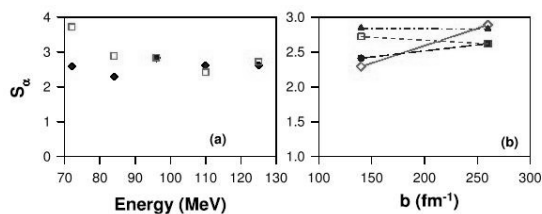


Fig. 7 The variation of alpha spectroscopic factor with respect to incident energy and single particle ANC.

5. Transfer Reaction and Elastic scattering to study cluster states

In previous sections the study of cluster states using breakup reaction has been studied. In this section we discuss the transfer reaction and elastic scattering methods. Though breakup reaction helps to measure the cluster states in a model independent way it is restricted to above threshold states only at present. For example, the two subthreshold states of ^{16}O viz. the 6.92 MeV (2^+) and the 7.12 MeV (1^-) states that play important role in the E1 and E2 capture of the $^{12}\text{C}(\alpha, \gamma)$ reaction at stellar energies (300 keV) cannot be studied so far by the breakup method. In this respect alpha transfer reactions on ^{12}C using $^{12}\text{C}({}^6\text{Li}, d)$ and $^{12}\text{C}({}^7\text{Li}, t)$ reactions have been utilized. The ANC of the two subthreshold states can be used to calculate the astrophysical S-factor of the $^{12}\text{C}(\alpha, \gamma)$ reaction at 300 keV. There are a number of angular distribution measurements above the barrier [36 and References therein] and only one total cross-section measurement deep below barrier [37]. The latter measurement claims an independence from the uncertain nuclear potentials involved in the DWBA calculations. However it has been shown recently [5] that total cross-section measurements are not sufficient and angular distributions deep below the barrier should be measured. In this work [5] the ANC extracted (using a near barrier data) for the 1^- state differs from that in [36] and [37] by almost an order of magnitude. There are however no angular distribution data below the barrier and we are planning such measurements. In the above barrier regime it is more difficult to extract the alpha spectroscopic properties. This is firstly due to the increased nuclear effects in the potential and secondly due to the presence of other reaction mechanisms such as the compound nuclear process. However, measurements above the barrier are easier due to increased cross-section and possibility of direct transfer may be more.

Recently measurements of the $^{12}\text{C}({}^6\text{Li}, d)$ reaction was performed at 20 MeV. The experiment

was carried out at the IUAC Pelletron, facility New Delhi. The angular distribution at these energies needs to be investigated in terms of nuclear potential sensitivity and multistep transfer process. Multistep transfer has been investigated at higher energy [38] for this reaction and so the present investigation at 20 MeV from this viewpoint may be fruitful. In fig.8 we show the angular distribution for the 6.92 MeV state and a representative Coupled Channel Born Approximation (CCBA) calculations using the code FRESKO.

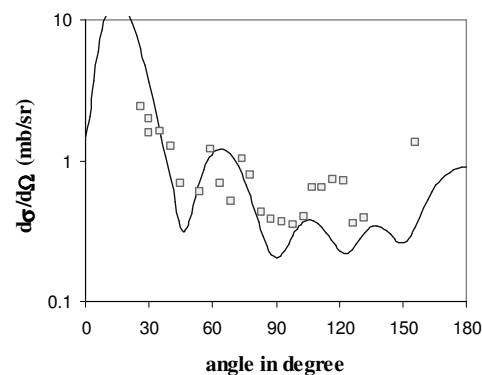


Fig. 8 Measured $^{12}\text{C}({}^6\text{Li}, d){}^{16}\text{O}^*$ (6.92 MeV) and CCBA calculations (solid line)

Measurement of elastic scattering resonances and phase shifts can be also used to study properties of cluster states in nuclei. This method has been used widely to study the alpha cluster states of ^{16}O using the $^{12}\text{C}(\alpha, \alpha')$ elastic scattering [4 and References therein] at low energies. So far we have discussed the clustering in light nuclei only. Alpha clustering in heavier nuclei is less known. In recent times [39 and references therein] quite a number of investigations have addressed the alpha clustering of ^{212}Po theoretically. Only one experiment [40] has been performed that report the alpha cluster states in ^{212}Po using alpha transfer reactions. It is also possible to study the cluster states from high energy elastic scattering. At higher energy if the alpha+ ^{208}Pb scattering data is analyzed then the corresponding potential can be obtained. This potential can then be used in the WKB Approximation to calculate the cluster states observed. A recent measurement of alpha+ ^{208}Pb in the energy region between 39-52 MeV has carried out at the VECC K=130 Cyclotron. In this energy regime there is no data in the literature. Fig.9 shows an analysis of the data in terms of folding model assuming the standard DDM3Y potential. Though the real potential satisfactorily explains the forward angle data the backward angle calculation is sensitive to the strength and type of the potential. This is being investigated and backward angle measurements are planned.

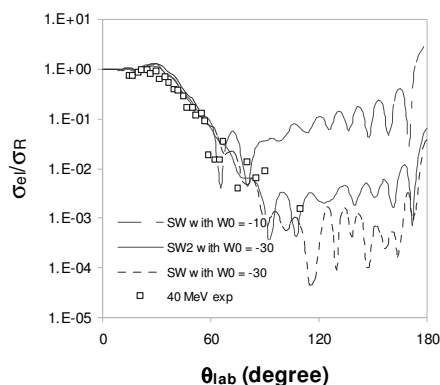


Fig. 9 Measured alpha+²⁰⁸Pb elastic scattering angular distribution at E(α)=40 MeV is compared with folding model calculation. The real potential is the standard DDM3Y potential. The imaginary potential is varied in strength and shape. SW signifies the Wood Saxon potential and SW2 represents the squared SW form factor.

6. Summary and Conclusions

We discuss the investigation of cluster states and its properties in nuclei using three different reactions. The alpha clustering is discussed as they are most common form of the phenomena. At first the breakup method and resonant particle spectroscopy is discussed. Experimental results from a RPS study of the ¹⁸O nucleus is presented in relation to its alpha+¹⁴C structure. Possible heavy ion constituents of the same nucleus are also studied. The spectroscopic properties of the ground and two unbound states of ¹⁶O is investigated in the framework of the CDCC theory. The importance of the results in relation to its application to nuclear astrophysics is elaborated. Similar studies have been extended to the case of ¹⁶O breakup from a light target. The transfer reaction and elastic scattering methods to study cluster states are also discussed in connection to recent measurements.

References

[1] W. von Oertzen, M. Freer and Y. Kanada-En'yo (2006) Physics Reports **43**, 432 (2006)
 [2] F. Hoyle, Astrophys. J. **1**, 121 (1954)
 [3] K. Ikeda, N. Takigawa and H. Horiuchi, Suppl. Prog. Phys. (Japan) Extra 464 (1969)
 [4] P. Tischhauser et al, Phys. Rev. C **79**, 055803 (2009)
 [5] Sucheta Adhikari and Chinmay Basu, Physics Letters B **704**, Issue 4 308 (2011)
 [6] Sucheta Adhikari and Chinmay Basu, Physics Letters B **682**, Issue 2 216 (2009)
 [7] W. D. Rae et al., Phys. Rev. Lett. **45**, 884 (1980)
 [8] W. D. M. Rae and R. K. Bhowmik, Nucl. Phys. A **420**, 320 (1984)

[9] W. D. Rae and R. K. Bhowmik, Nucl. Phys. A **427**, 142 (1984)
 [10] S. Yildiz et al., Phys. Rev. C **73**, 034601 (2006)
 [11] N. Curtis et al., Phys. Rev. C **66**, 024315 (2002)
 [12] N. I. Ashwood et al., J. Phys. G **32**, 463 (2006)
 [13] K. P. Artemov et al., Yad. Fiz. **37**, 1351 (1983)
 [14] S. Adhikari et al, Int. Jour. Mod. Phys. E Vol. **18**, No.9 1917 (2009)
 [15] FRESCO <http://www.fresco.org.uk>.
 [16] A.M. Mukhamedzhanov, N.K. Timofeuk, JETP Lett. **51**, 282 (1990)
 [17] R.E. Tribble, Nucl. Instrum. Methods Phys. Res. B **241**, 204 (2005)
 [18] L. Trache, et al., Phys. Rev. Lett. **87**, 271102 (2001)
 [19] N.C. Summers, F.M. Nunes, Phys. Rev. C **70**, 011602(R) (2004)
 [20] N.C. Summers, F.M. Nunes, Phys. Rev. C **78**, 011601(R) (2008)
 [21] F. Fleurot, et al., Phys. Lett. B **615**, 167 (2005)
 [22] M. Dufour, P. Descouvemont, Phys. Rev. C **78**, 015808 (2008)
 [23] C.E. Rolfs, W.S. Rodney, Cauldrons in the Cosmos, University of Chicago Press, 1988.
 [24] S. Adhikari and Chinmay Basu, Int. Jour of Mod Phys E Vol. **20**, No. 4 958 (2011)
 [25] D. Robson, Nucl. Phys. A **204**, 523 (1973)
 [26] J. Raynal, Notes on ECIS94, Report No. CEA-N-272, 1994, unpublished
 [27] B. Bonin, et al., Nucl. Phys. A **445**, 381 (1985)
 [28] J.Y. Hostachy, et al., Nucl. Phys. A **490**, 441 (1988)
 [29] C.A. Bertulani, Phys. Rev. C **49**, 2688 (1994)
 [30] K.L. Langanke, S.E. Koonin, Nucl. Phys. A **439**, 384 (1985)
 [31] D.R. Tilley, H.R. Weller, C.M. Cheves, Nucl. Phys. A **564**, 1 (1993)
 [32] P. Descouvemont, D. Baye, Phys. Rev. C **36**, 1249 (1987)
 [33] S.J. Padalino et al, Phys. Rev. C **41**, 594 (1990)
 [34] B.M. Levdev et al, Nucl. Phys. A **298**, 206 (1978)
 [35] A. Roy et al, Phys. Rev. C **20**, 2143 (1979)
 [36] A. Belhout, et al., Nucl. Phys. A **793**, 178 (2007)
 [37] C. Brune, et al., Phys. Rev. Lett. **83**, 4025 (1999)
 [38] N. Keeley et al, Phys. Rev. C **67**, 044604 (2003)
 [39] T. T. Ibrahim, S. M. Perez and S. M. Wyngaardt, Phys. Rev. C **82**, 034302 (2010)
 [40] A. Astier, P. Petkov, M.-G. Porquet, D. S. Delion, P. Schuck, Phys. Rev. Lett. **104**, 042701 (2010)